Published in final edited form as:

J Biomed Mater Res B Appl Biomater. 2011 October ; 99(1): 180–190. doi:10.1002/jbm.b.31885.

Hybrid coaxial electrospun nanofibrous scaffolds with limited immunological response created for tissue engineering

Jessica M. Gluck[1,2,3], **Paymon Rahgozar**[1], **Nilesh P. Ingle**[4], **Fironia Rofail**[1], **Asdghig Petrosian**[1], **Michael G. Cline**[1], **Maria C. Jordan**[2,3], **Kenneth P. Roos**[2], **William Robb MacLellan**[2], **Richard J. Shemin**[1], **Sepideh Heydarkhan-Hagvall**[1]

[1]Department of Surgery, Cardiovascular Tissue Engineering Laboratory, David Geffen School of Medicine, University of California, Los Angeles, California

[2]Department of Medicine, The Cardiovascular Research Laboratories, David Geffen School of Medicine, University of California, Los Angeles, California

[3]Department of Physiology, The Cardiovascular Research Laboratories, David Geffen School of Medicine, University of California, Los Angeles, California

[4]College of Textiles, North Carolina State University, Raleigh, North Carolina

Abstract

Electrospinning using synthetic and natural polymers is a promising technique for the fabrication of scaffolds for tissue engineering. Numerous synthetic polymers are available to maximize durability and mechanical properties (polyurethane) versus degradability and cell adhesion (polycaprolactone). In this study, we explored the feasibility of creating scaffolds made of bicomponent nanofibers from both polymers using a coaxial electrospinning system. We used a core of poly(urethane) and a sheath of a mixture of poly(ε-caprolactone) and gelatin, all dissolved in 1,1,1,3,3,3-hexafluror-2-propanol. These nanofibrous scaffolds were then evaluated to confirm their core–sheath nature and characterize their morphology and mechanical properties under static and dynamic conditions. Furthermore, the antigenicity of the scaffolds was studied to confirm that there is no significant foreign body response to the scaffold itself that would preclude its use *in vivo*. The results show the advantages of combining both natural and synethic polymers to create a coaxial scaffold capable of withstanding dynamic culture conditions and encourage cellular migration to the interior of the scaffold for tissue-engineering applications. Also, the results show that there is no significant immunoreactivity *in vivo* to the components of the scaffolds.

Keywords

coaxial; electrospinning; polycaprolactone; polyurethane; gelatin; tissue engineering

Correspondence to: S. Heydarkhan-Hagvall; shagvall@mednet.ucla.edu.

INTRODUCTION

Tissue engineering is a rapidly growing field of study that aims to repair, and/or replace damaged tissues and organs using a combination of structured scaffolds, specific cell types, and biologically active molecules. In general, the goal of tissue engineering is to mimic the endogenous three-dimensional (3D) environment of the target tissue as closely as possible. The natural extracellular matrix (ECM) is comprised of a complex network of structural and regulatory proteins that are arranged into a fibrous matrix. Development of 3D scaffolds that can recapitulate the natural ECM will allow cell attachment and migration as well as diffusion of nutrients, metabolites and soluble factors until the seeded cells can produce a new functional matrix and regenerate the desired tissue structures.[1–3] The ideal scaffold must satisfy a number of often conflicting demands: high porosity allowing for cell migration, sufficient surface area and a variety of surface chemistries that encourage cell adhesion, growth, migration, and has a degradation rate that closely matches regeneration rate of the desired natural tissue. Moreover, the scaffold must be biologically inert so as not to stimulate a foreign body response.

A broad range of tissue-engineering matrices have been fabricated from both synthetic and natural polymers using solvent casting and particulate leaching, gas foaming, freeze drying, rapid prototyping, thermally induced phase separating, fiber bonding, melt molding, and electrospinning, as reviewed elsewhere.[4–7] Electrospinning in particular has been used as an effective method to fabricate biomimetic scaffolds comprised of fibrous meshes. The process produces nonwoven scaffolds with a large network of interconnected pores that is conducive to tissue ingrowth. In conjunction with the porous network, small diameter fibers and high surface area to volume ratio in the electrospun scaffolds promote cell adhesion and migration as well as function as a delivery vehicle for biochemical signals needed for the seeded cells and efficient exchange of nutrients and metabolic waste.[8–10] Electrospinning has successfully been used in the fabrication of scaffolds made from many different polymers including poly(ε-caprolactone) (PCL), poly(lactic acid), poly(glycolic acid), poly(lactide-co-glycolide), and poly(urethane) (PU) in addition to the natural proteins, such as collagen, elastin and gelatin.[9–12]

Synthetic polymers provide many advantages over natural proteins due to price, availability and reliability.[13,14] They possess a wider range of mechanical properties than natural polymers and their lot-to-lot uniformity translates into the production of consistently uniform scaffolds. They can also be combined with natural proteins to produce hybrid scaffolds, which demonstrate beneficial properties of both starting materials. For example, the weak mechanical properties of natural proteins are overcome by combining them with a synthetic polymer, reinforcing the strength and durability of the scaffold while retaining the specific cell affinity of the natural polymer.[13] Many natural polymers exist such as gelatin, a natural biopolymer derived from collagen by controlled hydrolysis, which is a heterogeneous mixture of single or multistranded polymers. Gelatin has several potential advantages over other natural proteins, such as its biological origin, biodegradability, biocompatibility, and commercial availability at low cost.[15,16]

As with all tissue-engineered structures, the body's native tissue reaction to the implanted cell-scaffold construct can cause an immunogenic response. As such, it is necessary to limit that response as much as possible. Macrophage and foreign body giant cells play a crucial role in the foreign body reaction, and their responses toward implanted materials have significant impact on the proper functioning of medical devices. The formation of a fibrous capsule during the foreign body reaction is one of the most common barriers observed prohibiting normal function of medical devices, such as biosensors, drug delivery systems, eye implants, etc. Material surface chemistry, physical properties, and morphological features all play a part in modulating cellular reactions toward implant materials.[17–19]

In this study, we fabricated coaxial electrospun hybrid scaffolds, which combined synthetic materials with natural proteins to overcome limitations seen with scaffolds constructed with either one alone, such as poor cell adhesion and weak mechanical properties. We produced electrospun nanofibers composed of two distinct polymer solutions arranged in a core–sheath configuration. We used scaffolds made of bicomponent fibers with a gelatin–PCL mixture in the sheath and a PU core, which were determined to provide optimal fiber diameter, pore size and strength, leading to enhanced seeding of the electrospun scaffolds with cells *in vitro*. No immunogenic reaction to the fabricated scaffold was observed in this study *in vivo*. The mechanical properties of the scaffold should prove useful for their application in the field of cardiovascular tissue engineering and regenerative medicine.

MATERIALS AND METHODS

Scaffold fabrication

Unless otherwise noted all reagents were purchased from Sigma Aldrich (St. Louis, MO). In general, relatively volatile solvents are quite suitable for electrospinning polymeric fibers to ensure rapid drying of electrospun mats. We, like others, noted that 1,1,1,3,3,3-hexafluoro-2-propanol (HFP) is sufficiently volatile (Boiling Point 61°C) and has been used as a solvent in which proteins and simpler amino acid sequences have been suspended for various conformational analysis studies.[14] In this study, in order to create a customized electrospun scaffold, a solution of gelatin type B (bovine skin) (10% w/v) and PCL (10% w/v) and a solution of PCL alone (10% w/v) were dissolved in HFP. The solution was then loaded into a 10-mL syringe, to which an 18-gauge blunt ended needle (spinning nuzzle) was attached. A core solution of 5% w/v PU dissolved in HFP was loaded into a 3-mL syringe, to which a 25-gauge needle was attached. This syringe and needle was then loaded into the 10-mL syringe containing the sheath solution. The entire syringe system was then loaded into a modified syringe pump, as seen in Figure 1. The positive output lead of a high voltage supply (28 kV; Glassman High Voltage, NJ) was attached to the needle on the 10-mL syringe, spinning nuzzle. In the created electric field, a thin jet was ejected from the solution in the syringe at a speed of 70 μL/min from the raised syringe pump. The grounded target was placed 16 cm under the needle tip and upon introduction of the electric field Taylor cone formation at the base of the spinning nuzzle was observed. By the time the jet reached the target, a dry fiber was collected in the form of a flat 3D mat (300- to 400-μm thick). After the electrospinning process, the scaffold was then sterilized by soaking scaffolds for 30 min

in 70% ethanol, and then washed with sterile Dulbecco's phosphate-buffered saline (1×) before seeding with cells for *in vitro* or *in vivo* studies.

Ultrastructural scaffold analysis

Scanning electron microscopy.—For ultrastructural analysis, unseeded scaffold samples were processed for characterization by scanning electron microscopy (SEM) as described previously.[14] Fiber samples were cut from different, randomly selected locations on the electrospun mat to obtain representative fibers. The samples were mounted onto stubs and sputter coated with gold/palladium (Au/Pd to a thickness of ~ 10 μm) using Denton Desk II before scanning with a JEOL 6610 Low-Vacuum SEM (JEOL, Tokyo, Japan). Fiber diameters in the electrospun scaffolds were measured on scanning electron micrographs. Average fiber diameter was determined from measurements taken perpendicular to the long axis of the fibers within representative microscopic fields (20 measurements per field). The pores formed at the interstices of the fibers were measured using ImageJ software (free download available at http://rsbweb.nih.gov/ij/). For each sample, at least 5 scanning electron micrographs at 2000× magnification were used for image analysis and pore size measurement.

Transmission electron microscopy.—For transmission electron microscopy (TEM), polymer solutions were prepared for regular scaffold fabrication. Gold nanoparticles (GoldSol, Aurion, The Netherlands) of a 10 nm particle size were added to the sheath solution before electrospinning. After scaffold fabrication, scaffolds were embedded in Eponate 12 Resin (Ted Pella, Inc, Redding, CA) and sectioned with a Leica EM UC6 Ultramicrotome before scanning with a JEOL 100CX Transmission Electron Microscope. Images were analyzed using ImageJ software.

Contact angle measurement.—For contact angle measurement, the static sessile drop method (ASTM D7334–08 Standard Practice for Surface Wettability of Coatings, Substrates and Pigments by Advancing Contact Angle Measurement) was used with a goniometer to capture images of the scaffolds immediately after a 10 μL drop of water was applied to the surface of each scaffold.

Mechanical testing

Electrospun samples were cut into 40 × 10 mm^2 pieces, an average width:length ratio of 3:1, for mechanical testing. Scaffolds that were tested for degradation analysis were left in a dessicator for at least 72 h to ensure complete dryness before testing. Initial monotonic tensile testing was conducted on an Instron 5564 (Norwood, MA) using a 1 *N* load cell at a speed of 10 mm/min and a gauge length of ~ 30 mm with a pneumatic flat jaw clamp.

Cell seeding

Murine fibroblast NIH 3T3 (ATCC, CRL-1658) cells were cultured to a confluent state and at passage 4 were seeded onto the electrospun scaffolds at a density of 10^6 cells/cm^2 to reach a confluent cell layer. The 3T3-seeded scaffold was then cultured for 4 weeks under dynamic conditions in Dulbecco's modified Eagle's medium supplemented with 10% Fetal Bovine Serum (FBS) at 37°C and 5% CO_2.

Surgical procedure and implantation of scaffolds

UCLA Animal Research Committee approval (protocol # 2010–007-01) was obtained for all procedures. National Institute of Health (NIH) guidelines for the care and use of laboratory animals were observed. Four different groups -- coaxial, coaxial without gelatin (denoted as '*coaxial #2*'), porcine small intestine submucosa (SIS) scaffolds (Cook Medical, Bloomington, IN) and sham were tested at three different time points (2, 4, and 7 weeks). Coaxial #2 scaffolds were fabricated as previously described with the modification of no gelatin in the sheath polymer solution. Anesthesia was induced with 5% isoflurane and maintained with 2% isoflurane. Four 1 × 1 cm^2 sections of sterile scaffold from each group were cut and implanted in the lateral superior region of the subcutaneous dorsum, approximately one-third the distance between the head and tail, c57/BL6J male mice with an average weight of 30 g. Inflammation at the implant site, behavioral changes and other adverse reactions to the implant were monitored for the duration of the experiment and no significant abnormalities were observed. Sham control mice had a subcutaneous incision with no scaffold implant.

Tissue collection, histology and immunohistochemistry

On weeks 2, 4, and 7 postimplantation, the animals were euthanized and tissue was harvested. Following fixation, the tissue was then embedded in paraffin. Paraffin-embedded tissues were cut into 5-μm sections and stained for different histological analysis using hematoxylin and eosin (H&E) (American Mastertech, Lodi, CA), Masson's trichrome (American Mastertech, Lodi, CA).[14] CD 45 (BD Biosciences, dilution 1:100), a mouse monoclonal antibody, and IL-6 (Abcam, dilution 1:400), a rabbit monoclonal antibody were used for immunohistochemisty following standard protocols.[14] Fluorescence images were acquired using a confocal TCS SP2 AOBS laser scanning microscope system (Leica Microsystems, Exton, PA, http://www.leica.com) with 40× [1.3 numerical aperture]. Images were processed with Adobe Photoshop CS3 (Adobe Systems Inc., San Jose, CA, http://www.adobe.com).

To detect the cell attachment on the electrospun scaffolds as well as cell migration through the scaffolds *in vitro*, the scaffolds were analyzed at three time points, 7, 14, and 28 days in culture. Cell-seeded scaffolds were fixed in 4% formaldehyde and paraffin-embedded. To determine cell migration through the interior of the scaffolds, sections were cut in 5 μm thicknesses at a vertical cross-section, deparaffinized permeabilized with 0.5% Triton X-100 and nuclei stained with 4′-6-Diamidino-2-phenylindole (DAPI). To determine the extent of cell migration into the interior of the scaffold, the following equation was used:

$$M = (X/T) * 100 \quad (1)$$

where M is the percent migration, X is the distance migrated from the surface of the scaffold into the interior (as determined via DAPI staining), and T is the thickness of the scaffold.

Statistical analysis

Results are presented as mean±standard error of mean. Statistical significance was tested using Analysis Of Variance (ANOVA). Probability values of $P < 0.05$ were considered statistically significant.

RESULTS

Scaffold fabrication and morphology

Gelatin, PU, and PCL were dissolved in HFP and electrospun, either separately or mixed together. Previously, we have determined that a PCL-only scaffold does not sufficiently support cell growth and the addition of gelatin is necessary to promote cell adhesion qualities.[14] We have established in previous studies that a minimum polymer concentration is required for pure synthetic nanofibrous scaffold fabrication, thus a minimum polymer concentration of 5% PU was used[14] and 10% PCL–10% gelatin solution was chosen for the hybrid scaffold synthesis based on our previous work. We used these "standard" scaffolds to compare scaffolds prepared via the coaxial system. 5% PU concentration was used for the core of the coaxial system, and a 10% PCL–10% gelatin concentration was used for the sheath (Figure 1). SEM and TEM image analysis of the standard and bicomponent electrospun scaffolds showed a 3D nanofibrous mat of random fiber orientation (Figures 2 and 3).

Analysis of the images obtained from SEM (Figure 2) showed uniform fiber morphology for both the standard and coaxial electrospun scaffolds, regardless of needle configuration. However, upon visual observation of the SEM images the standard scaffolds had less fiber volume when compared to the coaxial scaffolds possibly secondary to increased variation in fiber diameter in the standard scaffolds, which is likely related to the development of multiple Taylor cones during the electrospinning process. TEM image analysis (Figure 3) confirms the existence of the core–sheath structure in the coaxial scaffolds. Gold nanoparticles were included in the sheath polymer solution to identify the outer sheath. These nanoparticles were visible in the electron micrographs as "black spots." The sheath layer is well delineated and no gold nanoparticles are seen within the core section.

Fiber diameter and pore size

The average fiber diameter and pore size of the various scaffolds are shown in Table I and Figure 4. As shown, the average fiber diameter was significantly smaller for the coaxial scaffolds as compared to the standard scaffold ($P < 0.001$). More specifically, the coaxial scaffolds had an average fiber diameter of 0.537 ± 0.053 μm, while the standard scaffolds had an average fiber diameter of 1.245 ± 0.113 μm. Consistent with these findings there were larger pore sizes and more variation of those pore sizes with the standard scaffolds (Figure 4). The contact angle of the standard scaffolds was 49.06 ± 1.77°, while the coaxial scaffolds had a contact angle of 51.67 ± 1.10°. Measurements were taken immediately after the drop was applied to the surface of the scaffold. Within 60 s, the water droplet was absorbed by both scaffolds, respectively. The scaffolds demonstrated similar hydrophilic properties predicting good cell adhesion properties.

Mechanical analysis

The stress and strain properties of the standard versus coaxial scaffolds are shown in Table I. The standard scaffold exhibited the lowest tensile stress value at 0.83 MPa, while the coaxial scaffold exhibited a peak stress of 1.67 MPa. The average strain at peak stress is also shown in Table I. The standard scaffold was only able to withstand a strain of 2.7%, while the coaxial scaffold demonstrated a strain of 36% at peak stress. While the mechanical properties of the two scaffolds demonstrated no significant difference, the coaxial scaffolds were significantly more stable under culture conditions and were able to retain all structural integrity as compared to the standard scaffolds, which lost structural and mechanical integrity after 7 days *in vitro*. As such, the standard scaffolds were not tested as part of a degradation study. After one week in culture, the standard scaffolds could not be physically handled for any volume, mass or tensile measurements (Figure 5 and Table II). The coaxial scaffolds exhibited an average volume retention compared to the original volume and mass measured before the samples were subjected to culture media and stored at 37°C of 76.71% after 1 week and 54.37% after 2 weeks in culture-like condition. Likewise the average mass retention was 73.20% after 1 week and 68.30% after 2 weeks in culture-like condition. After 2 weeks the volume and mass loss tapered off and remained steady for a total of 4 weeks. The tensile properties did drop dramatically after 1 week in culture-like condition (Table II): the modulus of the coaxial scaffolds dropped to 47.92 ± 2.82 MPa, the tensile strength dropped to 1.41 ± 0.14 MPa, and the strain dropped to 0.10 ± 0.018. After 1 week in culture-like condition, the tensile properties remained steady and did not continue to decrease significantly.

Cell–scaffold interactions

Cell–scaffold interactions were studied *in vitro* by seeding murine NIH 3T3 fibroblasts on both the standard and coaxial scaffolds for analysis at various time points. No additional surface modification of the electrospun scaffolds was necessary to ensure robust attachment of 3T3 cells to the scaffold. After 7 days in dynamic culture, cells began to migrate into the interior of the scaffolds (Figure 6).The cells seeded on the standard scaffolds migrated 21.0 ± 1.4% of the entire scaffold thickness, while cells seeded on the coaxial scaffolds migrated 17.6 ± 1.1% into the scaffold. After 14 days in culture, the standard scaffolds showed significant evidence of degradation and had begun to lose their structural and mechanical integrity, thus no cell migration measurements were possible. However the coaxial scaffolds retained their structural integrity and cells migrated 33.5 ± 1.7% and 31.0 ± 2.2% after 14 and 28 days respectively.

Immunogenicity of scaffolds

To determine the extent of the immune response to the electrospun scaffolds *in vivo*, scaffolds were inserted subcutaneously into mice and H&E staining was done on scaffolds explanted from the animals at 2, 4, and 7 week time points. SIS scaffolds are commonly used for many cardiovascular surgical procedures and were included as a benchmark for immune response levels and cellular infiltration. As depicted in Figure 7, nuclei staining is detected at 2 weeks in both electrospun scaffolds [Figure 7(A,D)], while there is almost no cellular infiltration at any time point for the implanted SIS scaffolds. Because we were

unable to detect any cell migration into the scaffold in the SIS scaffolds [Figures 7(G–I)], we did not anticipate finding any cellular ingrowth into the interior of the electrospun scaffolds. However, at later time points, cellular ingrowth of host cells is clearly visible in both the electrospun coaxial scaffolds with and without gelatin. The scaffold boundaries are readily detectable even at the 7 week time point (depicted by arrows, indicating scaffold boundaries), suggesting the slow degradation of the synthetic polymers used in the fabrication of the scaffolds. Immunological response to foreign bodies is often associated with fibrous capsule formation. This is easily detected by trichrome staining, which shows collagen deposition along the longitudinal axis of the implanted scaffold. As shown in Figure 8, relatively small fibrous capsules are seen around all scaffolds (Figures 8G–I, depicted as “FC”). Cellular ingrowth is visible at all time points in these scaffolds, suggesting the lack of structure of the fibrous capsules as barriers to the scaffolds. To further characterize the immunological response, we performed an immunohistochemical analysis of the scaffold for IL-6 expression or the presence of CD45 positive cells (Figure 9). No CD45 and IL-6 staining was observed suggesting the scaffolds elicit no immunological response.

DISCUSSION

In the present study we created and characterized hybrid coaxial electrospun scaffolds that incorported PU and PCL synthetic polymers as well as natural polymers to enhance cell adhesion and migration for future tissue-engineering applications. We compared these coaxial scaffolds to conventionally electrospun standard fibrous scaffolds. Coaxial scaffolds, at least theoretically, would incorporate the beneficial properties of all of its components. PU electrospun scaffolds have demonstrated extreme elasticity and better handling characteristics but poor cell adhesion and no degradability (data not shown). In contrast the hybrid polymer solution (10% PCL–10% gelatin) for the outer surface, is inherently stiffer, but has excellent cell adhesion qualities, as determined previously.[14] The mechanical properties of the coaxial scaffold were superior to that of the standard scaffold (Table I). While there are increased values for both the Young’s Modulus and tensile strength for the coaxial scaffolds as compared to the standard scaffolds, the differences are not significant. A significant difference exists between the strain properties of the two scaffolds. The coaxial scaffolds exhibit a much higher elastic potential than the standard scaffolds. Overall, the inclusion of PU in our system adds the necessary elasticity to the mechanical properties of our scaffolds. Additionally, the inclusion of PU to the core of the scaffolds helps to maintain the structural and mechanical integrity for long-term studies both *in vitro* and *in vivo*. Likewise, the coaxial scaffolds exhibited superior handling and structural integrity after one week in culture-like conditions (Figure 5). The standard scaffolds fell apart during the transfer out of the culture dish to be measured for volume and mass retention. As such, these scaffolds were not included in further degradation or *in vivo* studies. Additionally, after one week of culture-like conditions, SEM image analysis of the standard scaffolds showed no distinguishable fiber boundaries (data not shown). The morphology of the fibers of the coaxial scaffolds observed through SEM image analysis showed no significant difference in fiber diameter or pore size at each time point (data not shown). The coaxial scaffolds did show signs of degradation after one week in culture. The tensile properties of the scaffolds

dropped significantly, but remained steady for the remaining three weeks of the degradation study. The slow degradation was again visible during the *in vivo* studies, as the scaffold borders were still visible in the histological analysis (Figures 7 and 8).

While both scaffolds have exhibited similar tensile strength, the standard scaffolds demonstrated higher initial cell migration into the interior of the scaffold. However, this migration could not be sustained as the mechanical and structural integrity of the scaffold degraded quickly in aqueous conditions. The longer the scaffolds are submersed in liquid, the less stable they become and gross handling of the scaffolds is impossible without imparting damage to the structure of the scaffold. However, the coaxial scaffolds support less initial migration into the scaffold, but keep their mechanical integrity *in vitro* for at least 28 days. We believe the difference in migration capabilities resides in the differences in fiber diameter and pore sizes. Future work will include fabricating coaxial scaffolds with larger fiber diameters and consequently larger pore sizes (by varying the distance between needle tip and collection plate as well as flow rate), which we will expect to support even better cellular ingrowth.

Scaffolds were implanted subcutaneously to ascertain the extent of immunological response in the murine host. Due to the poor handling and obvious mechanical deterioration of the standard scaffolds over longer time points, we were not able to include these in the *in vivo* study as we were unable to implant the scaffolds in the animals. In addition, we used coaxial scaffolds with no gelatin in the sheath polymer solution to determine if any immunological response would be mounted due to the species difference of the bovine source of gelatin implanted in the murine host. These scaffolds were denoted "*coaxial #2*" The scaffold morphology was almost identical to that of the coaxial scaffolds with gelatin. Likewise, the mechanical analysis of the coaxial #2 scaffolds without gelatin was very similar to that of the coaxial scaffolds with gelatin (data not shown). SIS scaffolds, which are Food and Drug Administration (FDA)-approved and used in various surgical procedures routinely, were included as a guideline to demonstrate acceptable immunological response.

Soft tissue response to porous and fibrous biomaterials is influenced, in part, by the microarchitecture of the implant.[20,21] For porous materials like our electrospun scaffolds, effects of change to the pore size have been studied, suggesting that pore size dimensions of at least 10 μm are needed to allow connective tissue ingrowth and to avoid global encapsulation. The fabricated electrospun scaffolds clearly have pore sizes < 10μm (Figure 4) and we correctly anticipated the scaffolds to support at least minimal cell migration *in vitro*. Cellular infiltration has rarely been reported on electrospun nanofibers which usually demonstrate a two-dimensional behavior as the distance between layers of fibers is too small to allow cells to migrate through the scaffold without being impinged upon by a layer of fibers underneath the surface layer, thus preventing cellular infiltration. However, as seen in Figures 7 and 8, cellular infiltration did occur in the interior scaffolds in both the *in vitro* and *in vivo* studies. Interestingly, we observed a greater cell migration from *in vivo* studies than those observed in the *in vitro* studies. Given that the scaffolds were implanted with no cells seeded, the infiltrating cells are clearly those of the murine hosts.

The formation of the fibrous capsule is dependent upon both the physical and mechanical properties of the implanted biomaterial and the thickness of the fibrous capsule can have a significant influence on the functionality of the implant. Scaffolds with smaller pore sizes and a high surface area-to-volume ratio are more likely to induce dense fibrous capsule formation, thus the thickness of the fibrous capsules can be greatly reduced when implants are more porous with larger pore sizes, in turn promoting greater cellular ingrowth.[22,23] As we observed in Figure 8, the fibrous capsule formation around the periphery of both our fabricated electrospun scaffolds and commonly used, commercially available SIS scaffolds was minimal (as depicted by “FC” in Figure 8). The presence of native cells in the interior of the scaffold with a small fibrous capsule formation suggests the bovine source of gelatin in the sheath component of the electrospun scaffolds does not elicit a strong immunological response.

As seen in Figure 9, we observed a limited immune response with nearly no macrophage or common immunological marker present. Interleukin (IL) 6 was not clearly detected at any of the time points of the implanted electrospun scaffolds. Similarly, CD45 a common immunological marker was not detected in any of the implanted scaffolds. We can conclude that not only does the bovine source of gelatin not cause an immune response, but neither do the scaffolds themselves. We can also conclude the architecture of the electrospun scaffolds readily supports cell migration and can be used for further tissue-engineering applications.

CONCLUSION

ECM consists of a complex network of structural and regulatory proteins *in vivo*. The multifunctional nature of natural ECM will need to be considered in the design and fabrication of tissue-engineered scaffolds. The introduction of a protein/polymer hybrid such as PCL–gelatin or a coaxial system to include a core of PU and a sheath of PCL–gelatin provides both favorable mechanical properties and binding sites for cell attachment and proliferation. We anticipate these coaxially electrospun scaffolds to prove extremely useful for tissue-engineering applications, particularly those applications which will be used under dynamic conditions. The added elasticity and handling properties from the inclusion of PU to the core of the scaffolds will be extremely beneficial for future cardiovascular tissue-engineering applications. We believe electrospinning with natural and synthetic polymers can be used to produce tissue-engineered scaffolds for various applications. These scaffolds better recapitulate key features of the native ECM including its mechanical and biochemical properties. We can conclude the physical properties of our electrospun scaffolds are not only adequate in both fiber diameter and pore size, but will encourage and promote cellular migration and proliferation within the interior of the scaffold. By detecting robust native cell migration into the interior of the scaffold and observing minimal fibrous capsule formation and immunological response *in vivo*, we are confident our electrospun coaxial scaffolds will support further tissue-engineering studies.

Acknowledgments

The authors thank Mrs. Alicia Thompson at Center for Electron Microscopy at USC, Dr. Matt Schibler at CNSI at UCLA, and both Ms. Sanaz Heydarkhan and Ms. Mackenzie Postel for technical assistance.

Contract grant sponsor: Ruth L. Kirschstein National Research Service Award; contract grant number: T32HL69766 (to J.M.G.) and CIRM RB101354 (to W.R.M.).

Contract grant sponsor: Department of Cardiothoracic Surgery at UCLA

REFERENCES

1. Langer R, Vacanti JP. Tissue engineering. Science 1993;260: 920–926. [PubMed: 8493529]
2. Vacanti JP, Langer R. Tissue engineering: The design and fabrication of living replacement devices for surgical reconstruction and transplantation. Lancet 1999;354 (Suppl 1):S132–S134.
3. Narem RM. Tissue engineering: Confronting the transplantation crisis. Proc Inst Mech Eng 2000;214:95–99.
4. Ma PX. Scaffolds for tissue fabrication. Mater Today 2004;7:30–40.
5. Hou QP, Grijpma DW, Feijen J. Porous polymeric structures for tissue engineering prepared by a coagulation, compression moulding and salt leaching technique. Biomaterials 2003;24: 1937–1947. [PubMed: 12615484]
6. Piskin E Biodegradable polymers in medicine In: Scott G, editor. Degradable Polymers: Principles and Applications. Kluwer: Dordrecht; 2002 321 p.
7. Fambri L, Migliaresi C, Kesenci K, Pis_kin E. Biodegradable polymers In: Barbucci R, editor. Integrated Biomaterials Science. Kluwer: New York; 2002 119 p.
8. Guan J, FK, Sacks MS, Wagner WR. Preparation and characterization of highly porous, biodegradable polyurethane scaffolds for soft tissue applications. Biomaterials 2005;26:3981–3971. [PubMed: 15626445]
9. Khil MS, BS, Kim HY, Kim SZ, Lee KH. Novel fabricated matrix via electrospinning for tissue engineering. J Biomed Mater Res B Appl Biomater 2005;15:117–124.
10. Li WJ, LC, Caterson EJ, Tuan RS, Ko FK. Electrospun nanofibrous structure: A novel scaffold for tissue engineering. J Biomed Mater Res 2002;60:613–621. [PubMed: 11948520]
11. Boland ED, Matthews JA, Pawlowski KP, Simpson DG, Wnek GE, Bowlin GL. Electrospinning collagen and elastin: Preliminary vascular tissue engineering. Front Biosci 2004;9:1422–1432. [PubMed: 14977557]
12. Theron SA, Zussman E, Yarin AL. Experimental investigation of the governing parameters in the electrospinning of polymer solutions. Polymer 2004;45:2017–2030.
13. Liang D, Hsiao BS, Chu B. Functional electrospun nanofibrous scaffolds for biomedical applications. Adv Drug Deliv Rev 2007; 59:1392–1412. [PubMed: 17884240]
14. Heydarkhan-Hagvall S, Schenke-Layland S, Dhanasopon AP, Rofail F, Smith H, Wu BM, Shemin RJ, Beygui RE, MacLellan WR. Three-dimensional electrospun ECM-based hybrid scaffolds for cardiovascular tissue engineering. Biomaterials 2008;29:2907–2914. [PubMed: 18403012]
15. Rose P Encyclopedia of polymer science and engineering. 1987, New York: Wiley
16. Johns P, CA. The science and technology of gelatin. London: Academic; 1977.
17. Anderson JM, Rodriguez A, Chang DT. Foreign body reaction to biomaterials. Semin Immunol 2008;20:86–100. [PubMed: 18162407]
18. Ratner BD. Reducing capsular thickness and enhancing angiogenesis around implant drug release systems. J Control Release 2002;78:211–218. [PubMed: 11772462]
19. Anderson JM. Biological responses to materials. Ann Rev Mater Res 2001;31:81–110.
20. Von Recum AF, Van Kooten TG. The influence of microtopography on cellular response and the implications for silicone implants. J Biomater Sci Polym Edn 1995;7:181–198.
21. Campbell CE, Von Recum AF. Microtopography and soft tissue response. J Invest Surg 1989;2:51–74. [PubMed: 2487399]
22. Jansen JA, von Recum AF, van der Waerden JP, De Groot K. Soft tissue response to different types of sintered metal fibreweb materials. Biomaterials 1992;13:959–968. [PubMed: 1477267]
23. Hulbert SF, Morrison SJ, Klawitter JJ. Tissue reaction to three ceramics of porous and non-porous structures. J Biomed Mater Res 1972;6:347–374. [PubMed: 4116127]

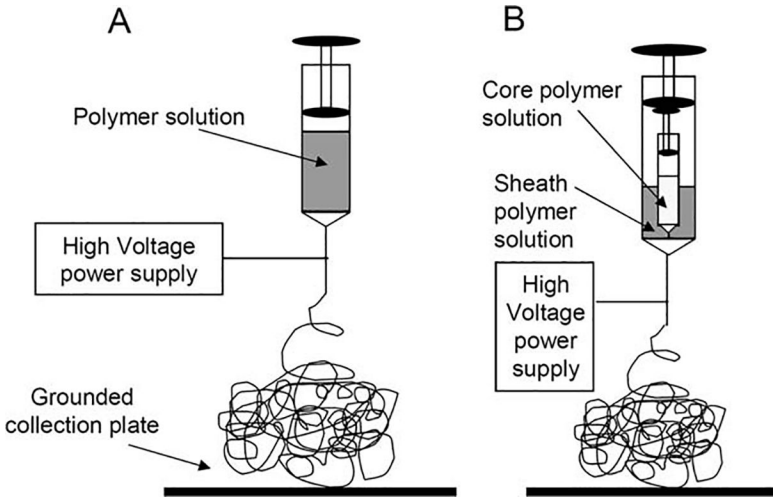

FIGURE 1.

Creation of nanofibrous scaffolds. A) Schematic of standard/unicomponent system for electrospinning B) Schematic of two-syringe system for electrospinning coaxial scaffolds.

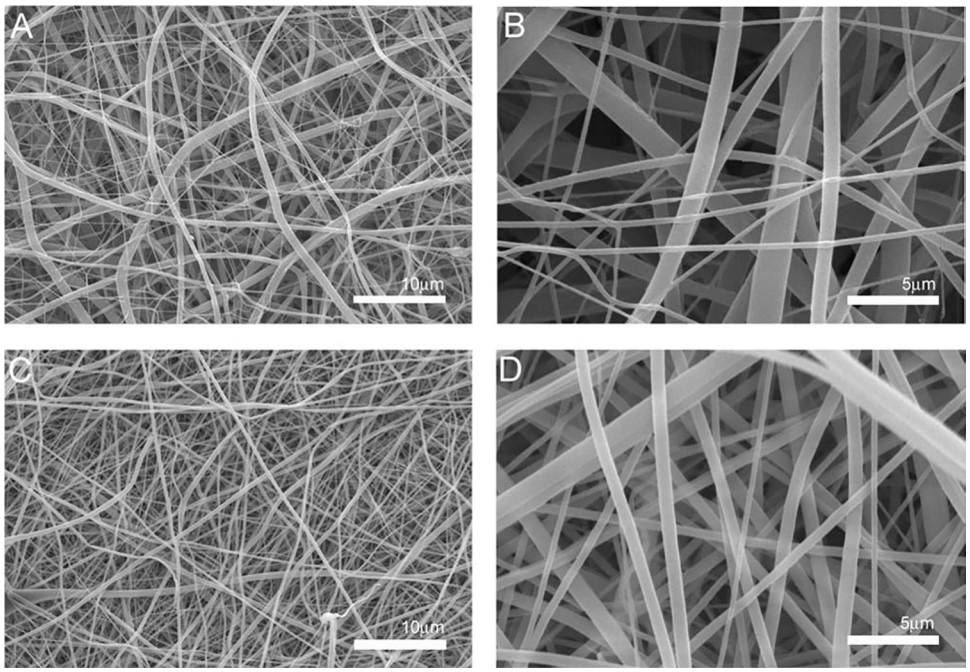

FIGURE 2.

Representative SEM micrographs of electrospun scaffold morphology. A) Standard 10% PCL-10% gelatin scaffolds at 1,000x with an average fiber diameter of 1.245 ± 0.413μm B) Standard scaffolds at 5,000x C) Coaxial scaffold at 1,000x with an average fiber diameter of 0.537 ± 0.231μm D) Coaxial scaffold at 5,000x. Scale bar equals 10μm A and C, Scale bar equals 5μm B and D.

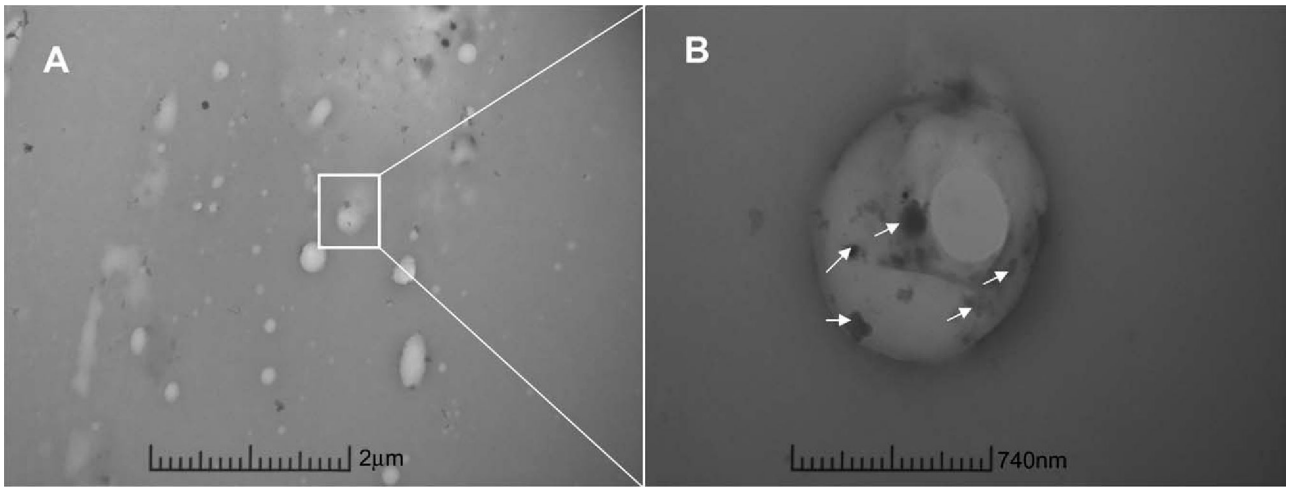

FIGURE 3.

Representative TEM micrographs of electrospun scaffold morphology. A) TEM micrograph of cross-section of bicomponent nanofibers in the coaxial scaffold. Outer sheath contains gold nanoparticles (small black dots, arrows) to distinguish from inner core. Scale bar = 2μm. B) Further magnification of cross-section of bicomponent nanofiber of coaxial scaffold. Arrows indict gold nanoparticle presence in sheath of fiber. Scale bar = 740nm.

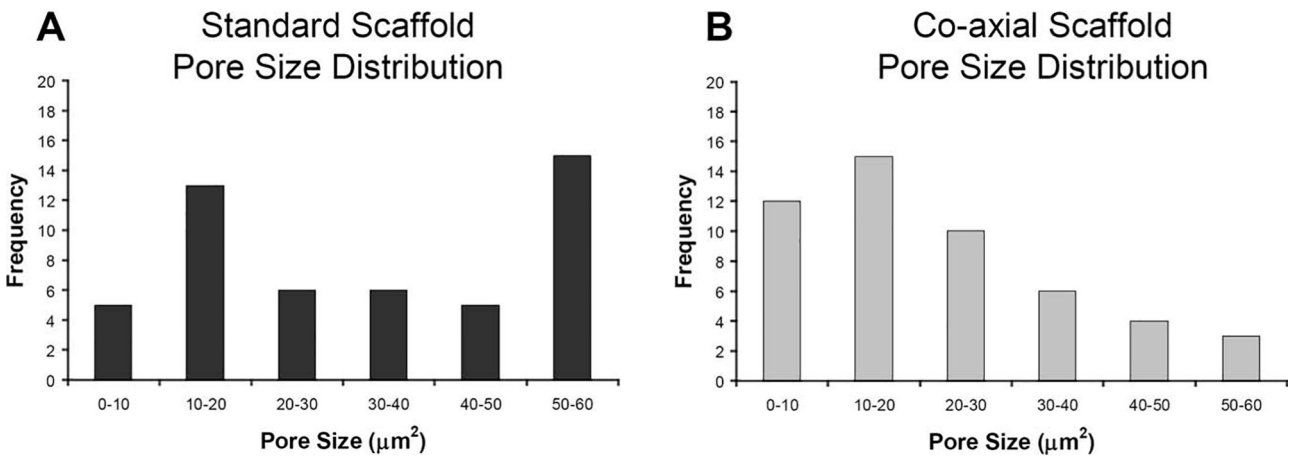

FIGURE 4.

Pore size distribution of standard and coaxial scaffolds. A) Pore size distribution of standard scaffolds with an average fiber diameter of 1.245 ± 0.413μm B) Pore size distribution of coaxial scaffold with an average fiber diameter of 0.537 ± 0.231μm.

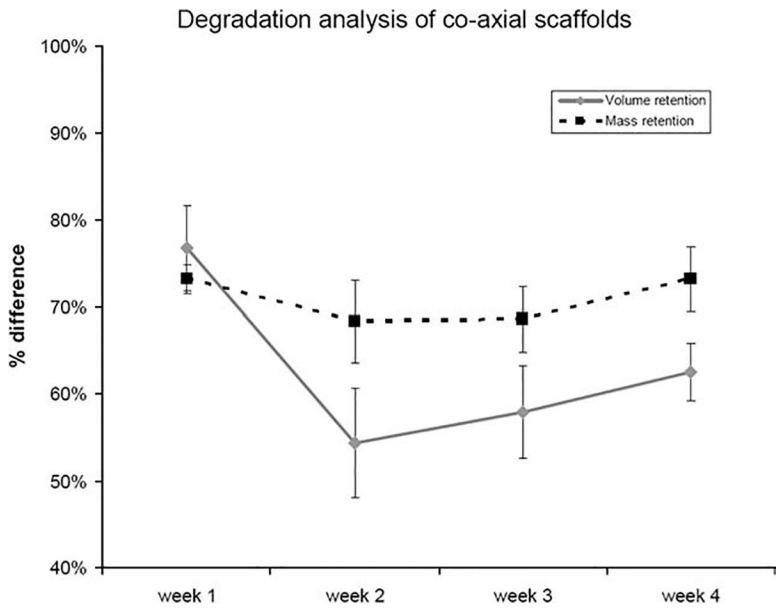

FIGURE 5.

Degradation analysis of electrospun scaffolds over four weeks. Volume and mass retention of coaxial scaffolds.

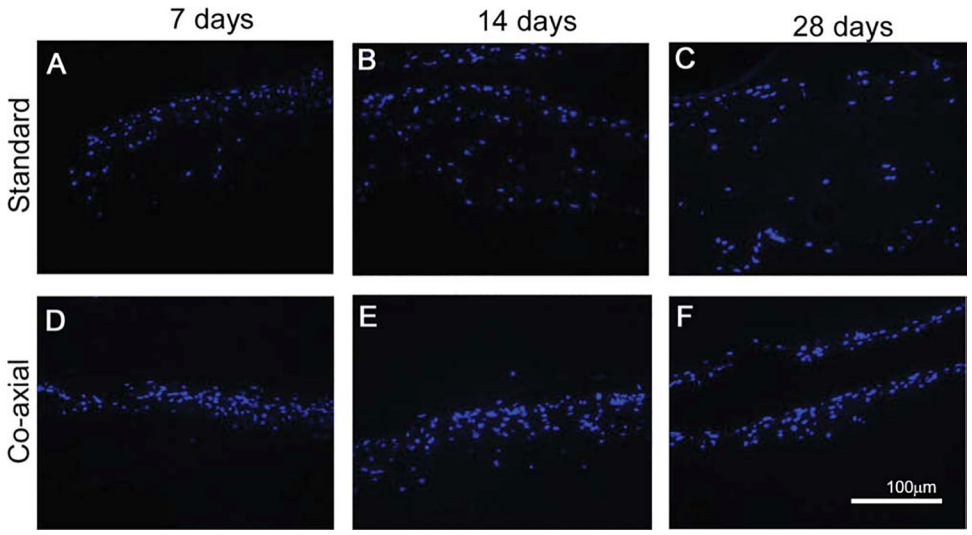

FIGURE 6.

3T3 cells seeded on scaffolds for 7,14, and 28 days. Nuclei stained (DAPI) NIH 3T3 fibroblasts cultured on **A-C**) Standard scaffolds, **D-E**) Coaxial scaffolds, scale bar = 100μm. [Color figure can be viewed in the online issue, which is available at wileyonlinelibrary.com.]

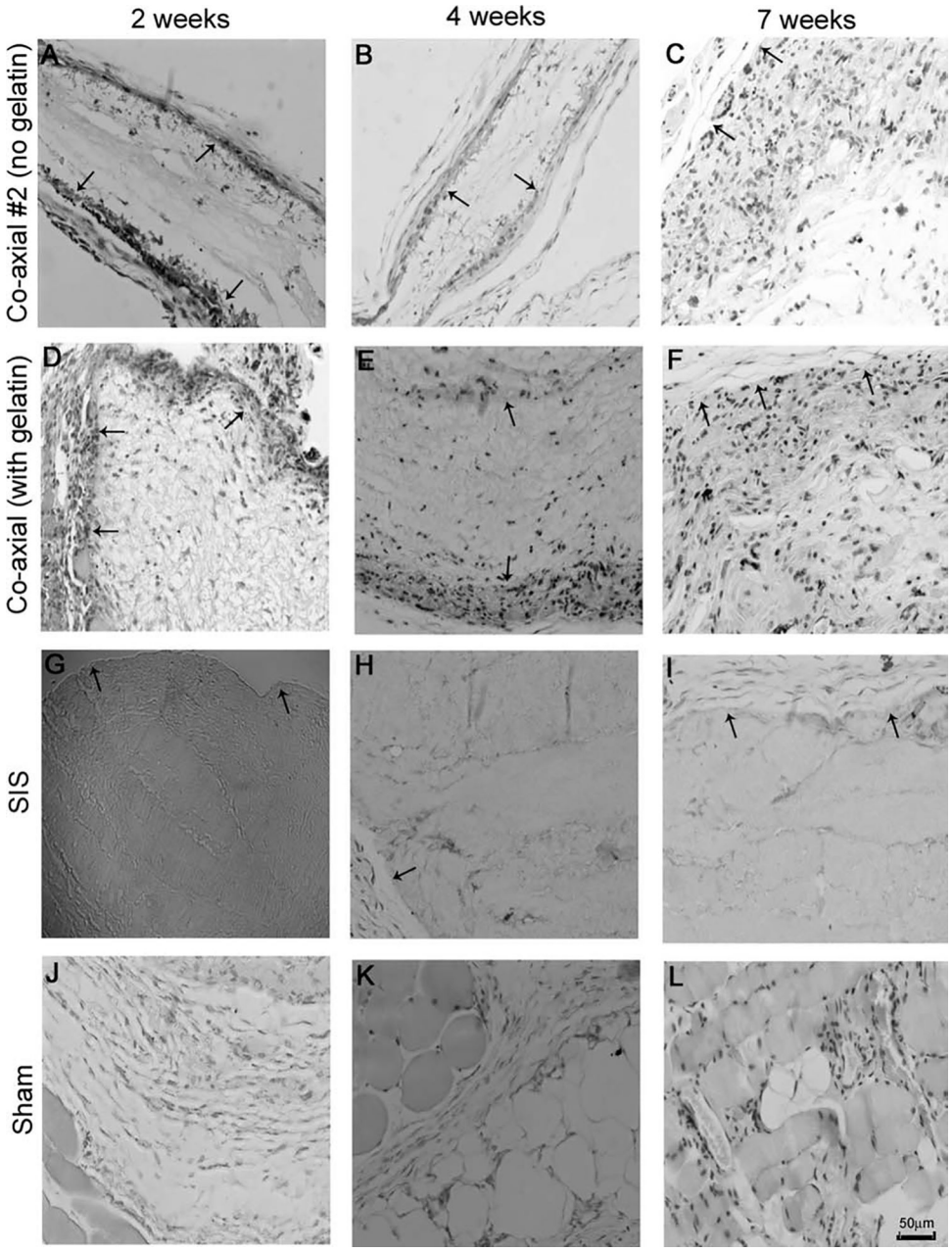

FIGURE 7.

H&E staining of implanted scaffolds at 2, 4, and 7 weeks. Tissue sections stained with hematoxylin and eosin reveals cellular ingrowth of native cells into electrospun scaffolds (original magnification 20x, scale bar = 50 μm). **A-C**) Coaxial #2 at 2, 4 and 7 weeks respectively. **D-F**) Coaxial at 2, 4, and 7 weeks. **G-I**) SIS scaffolds at 2, 4, and 7 weeks, **J-L**) Sham at 2, 4, and 7 weeks. Arrows indicate scaffold boundaries.

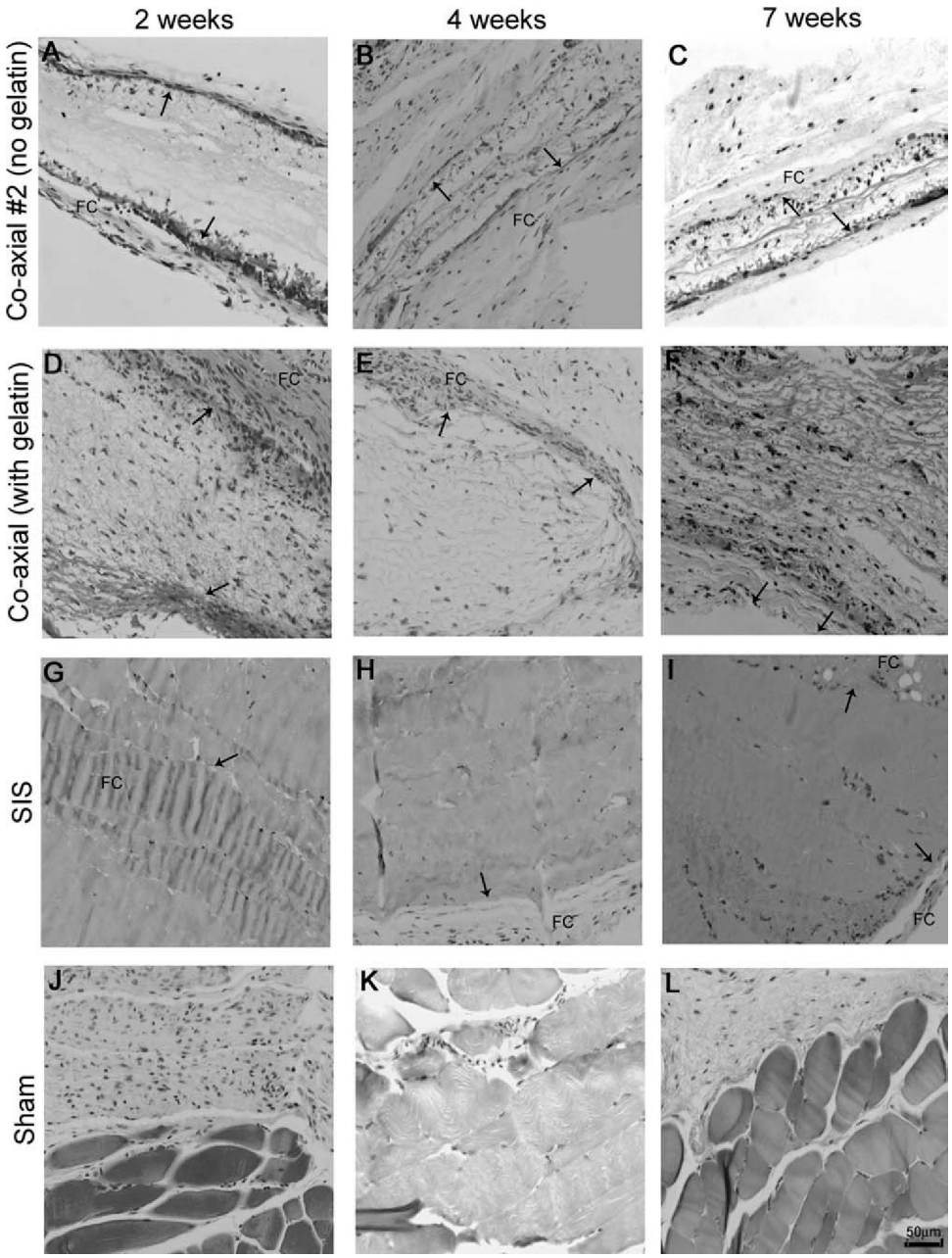

FIGURE 8.

Masson's trichrome staining of implanted scaffolds at 2, 4, and 7 weeks. Tissue sections stained with Masson's trichrome shows minimal fibrous capsule (FC) formation of electrospun and SIS scaffolds (original magnification 20x, scale bar = 50 μm). **A-C**) Coaxial #2 at 2, 4 and 7 weeks respectively. **D-F**) Coaxial at 2, 4, and 7 weeks. **G-I**) SIS scaffolds at 2, 4, and 7 weeks, **J-L**) Sham at 2, 4, and 7 weeks. Arrows indicate scaffold boundaries.

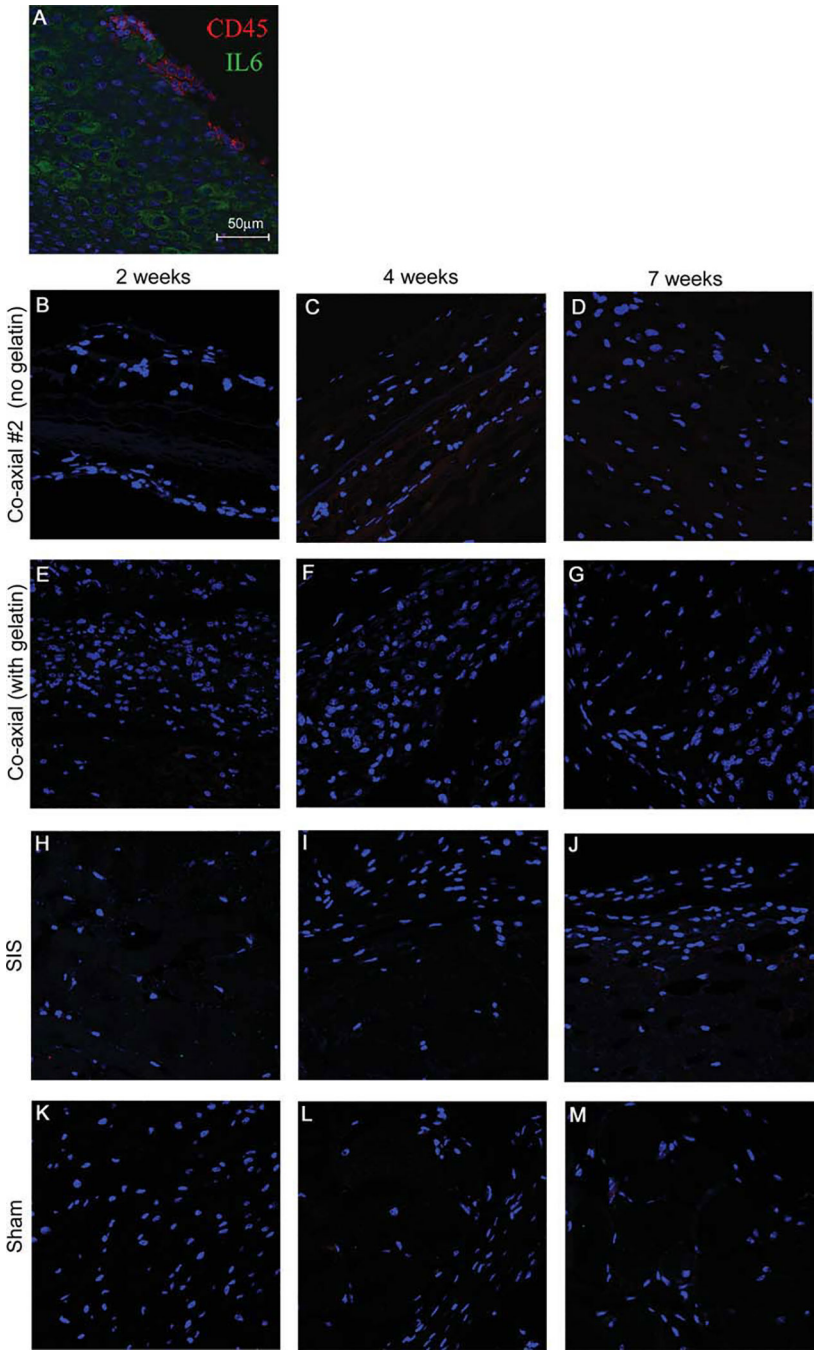

FIGURE 9.

Immunofluorescence staining of implanted scaffolds at 2, 4, and 7 weeks.

Immunohistochemistry staining of implanted scaffolds to detect immunological response by staining for markers CD45 (red) and IL6 (green) and DAPI (blue). **A**) positive control tonsil tissue. **B-D**) Coaxial #2 at 2, 4 and 7 weeks respectively. **E-G**) Coaxial at 2, 4, and 7 weeks. **H-J**) SIS scaffolds at 2, 4, and 7 weeks. **K-M**) Sham at 2, 4, and 7 weeks. Scale bar = 50

μm. [Color figure can be viewed in the online issue, which is available at wileyonlinelibrary.com.]

TABLE I.

Fiber Size and Mechanical Analysis of Electrospun Scaffolds

Scaffold	Avg. Fiber Diameter (μm)	Young's Modulus (MPa)	Tensile Strength (MPa)	Strain
Standard	1.245 ± 0.113	76.80 ± 14.66	0.83 ± 0.25	0.027 ± 0.013
Coaxial	0.537 ± 0.053	93.36 ± 9.11	1.67 ± 0.47	0.36 ± 0.054 *

TABLE II.

Mechanical Analysis of Coaxial Scaffolds Over 4 Weeks

	Week 0	Week 1	Week 2	Week 3	Week 4
Young's modulus (MPa)	93.36 ± 9.11	47.92 ± 2.82	47.99 ± 10.28	46.91 ± 6.99	40.43 ± 3.98
Tensile strength (MPa)	1.67 ± 0.47	1.41 ± 0.14	1.42 ± 0.19	1.63 ± 0.11	1.29 ± 0.08
Strain	0.36 ± 0.05	0.10 ± 0.02	0.12 ± 0.05	0.15 ± 0.02	0.13 ± 0.01